OPEN

Correspondence and
requests for materials
should be addressed to
Z.F.Z. (zhfzhang@imr.
ac.cn)

Intrinsically higher fatigue cracking resistance of the penetrable and movable incoherent twin boundary

L. L. Li, P. Zhang, Z. J. Zhang & Z. F. Zhang

Shenyang National Laboratory for Materials Science, Institute of Metal Research, Chinese Academy of Sciences, 72 Wenhua Road, Shenyang 110016, P.R. China.

Incoherent twin boundaries (ITBs) are widespread and play a crucial role in unidirectional deformation behavior of materials, however, the intrinsic role of individual ITB under cyclic loading remains elusive. Here we show the fatigue cracking behavior of Cu bicrystal with an ITB as its sole interface for the first time. The slip bands (SBs) could transfer through the ITB; meanwhile, the ITB could migrate with the motion of partial dislocations. Both the penetrability and mobility contribute to the higher fatigue cracking resistance of the ITB and hence the fatigue crack nucleates along the SBs preferentially. These new findings not only shed light on the fatigue cracking mechanisms of a penetrable boundary with direct evidence but also could provide important implications for future interfacial optimization of metallic materials.

I n recent years, coherent twin boundary (CTB) in face centered cubic (fcc) metals has drawn considerable interest. The incorporation of nanoscale CTBs can improve the strength and ductility synchronically by hindering the dislocation motion and providing ample room for dislocation accumulation[1–4]. There are inherently extensive steps and curvature which comprise partial dislocations bonded with CTBs[2,5,6]. And a softening phenomenon occurred when the twin thickness decreases below a critical value due to the existence of the preexisting dislocation sources and their easy slip along the CTBs[2,4,7–9]. Indeed, the defects along the CTBs could be identified as incoherent twin boundaries (ITBs). Both of experimental and simulation studies show that the $\Sigma3\{112\}$ ITB can be presented with a set of Shockley partial dislocations[7,10] and it can dissociate into two tilt walls bounding a 9R phase during the deformation[7,9,11,12]. In addition, the collective glide of the partial dislocations could lead to the CTB or ITB migration, twinning or detwinning during the deformation which contribute to the good ductility[7–9,12–15].

On the other hand, it is already known that random high-angle grain boundary (GB) rather than the penetrable low-angle GB is always the preferential fatigue cracking site[16–18]. And whether the CTB cracks or not depends on the orientation and stacking fault energy[19]. Apparently, the ITB is a special kind of high-angle GB which differs from conventional high-angle GB or CTB. There is lattice dislocation transmission across the ITB[20] and it is clear that due to the crystallographic specialty, the slip parallel to the CTB in the matrix and twin grains can transfer through the ITB. However, how the penetrable and movable ITB behaves during cyclic deformation is rarely studied and it is an intriguing and significant issue to be addressed. The ITB is widespread in fcc metals and generally bonded with the CTB, which could be created from electrodeposition[1], severe plastic deformation[21], phase transformation and recrystallization of deformed structures. The complex stress state in polycrystals obscures the original role of each microstructural unit. Thus a Cu bicrystal with one ITB as its sole internal boundary was employed and it was well designed to have the highest shear stress applied parallel to the CTB plane. Under this circumstance, same dislocation slips could operate in the component grains and the partial dislocations constructing the ITB are also capable of gliding. Then it was cyclically deformed to investigate the fatigue cracking behavior of individual ITB and it was expected to further expand our knowledge on interfacial optimization for future material design.

Results

The crystallographic orientation of the specimen is shown in Fig. 1. The ITB is the sole boundary in the bicrystal specimen as sketched in Fig. 1b. The GB and inverse pole figure (IPF) map of the specimen is shown in Fig. 1a and it could be seen that the boundary is not always straight across the whole specimen. The {111} pole figure is shown in Fig. 1b and it could be derived that there is twinning relationship between the two component grains. The black
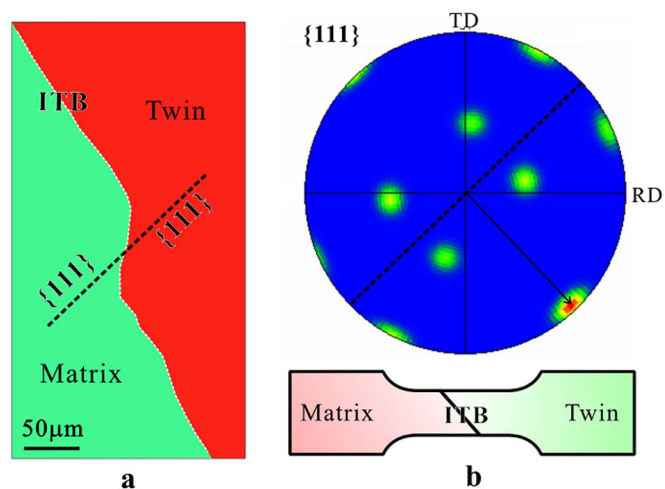
Figure 1 | The crystallographic orientation and sketch of the bicrystal specimen. (a) The GB + IPF map with (b) the corresponding {111} pole figure with the sketch of the bicrystal specimen with an ITB.

dashed lines in Fig. 1a and Fig. 1b represents the common {111} lattice plane, that is the theoretical twinning plane. This result confirms that the interface between the twin and matrix grains is an ITB. The bicrystal was specially designed that the shear stress is the highest along the common slip plane (CTB plane) in both component grains, wherein, the Schmid factors are 0.49 and 0.48, respectively in the two component grains.

The surface deformation morphology of the fatigued bicrystal is displayed in Fig. 2. The macroscopic morphology shown in Fig. 2a demonstrates that slip bands (SBs) are continuous across the ITB. More specifically, the SBs are continuous across both of the straight and curved ITBs as shown in Fig. 2b and Fig. 2c respectively with higher magnifications. The SBs could pass through the ITB on the four surfaces of the specimen, which appears like the slip morphology of the single-slip Cu single crystals or that containing low-angle GBs[22]. The representative fatigue cracking morphology is exhibited in Fig. 2d with an arrow pointing at the SB crack which broke through the ITB. Generally, there would be abundant secondary SBs in the GB affected zone (GBAZ) and the fatigue crack preferentially nucleated at the GB[16,22] during the cyclic deformation.

Unexpectedly, there were very few secondary SBs operated near the ITB and the fatigue cracks initiated along the SBs firstly similar to the single crystal[23] and could be observed on the four surfaces.

The subsurface dislocation arrangements of the fatigued bicrystal are shown in Fig. 3. Fig. 3a displays the typical dislocation veins and ladders in the component grains which correspond with the surface sparse SBs. And there is good continuity of the dislocation arrangement across the ITB which agrees with the surface SBs penetrating the ITB. At regions with dense SBs near the ITB, the dislocation arrangements are dominated by dislocation cells as depicted in Fig. 3b and Fig. 3c. Since an inverted imaging mode using a back-scattered electron detector was adopted, the ECC (electron channeling contrast) imaging is comparable to the transmission electron microscopy (TEM) observation[24]. Different contrasts stand for different dislocation densities or different crystallographic orientations. Obviously, the GB or ITB separating two grains should not separate one dislocation cell. Commonly, the dislocation walls would terminate at the rigid high-angle GB which prevents the dislocation motion from forming a complete cell[25]. On the contrary, the fatigued ITB is rugged at the microscale which becomes a part of the cell boundaries as the white dashed line represented in Fig. 3b and Fig. 3c. Some local fragments of the fatigued ITB are hard to be detected as indicated by the white dashed ellipse in Fig. 3d. The SB cracks could still be visible after grinding and electropolishing as those bright white ribbons shown in Fig. 3b and Fig. 3d.

Discussion

Due to the special crystallographic orientations, the slip systems with the highest Schmid factors on both sides of the ITB have the same slip planes and slip vectors as depicted in Fig. 4a. The active slip planes in the component crystals have the same intersecting lines with the boundary and the slip vectors have no divergence, which greatly favors the slip continuity across ITB[26]. Therefore, the slips could transfer through the boundary geometrically. In Cu bicrystal with a near-penetrable high-angle GB, there is 13.8° divergence between the slip directions on the identical slip planes of the SBs in both grains[22] and hence the slip could not pass through the GB. The fatigue crack preferentially nucleated at the GB[16,22] eventually, which implies that the strain compatibility near the GB is not as good as that near the ITB. In addition, the lattice dislocations could transfer through the ITB by interacting with the ITB partials as displayed in Fig. 4b. The red symbols at the ITB represent the partials constructing the
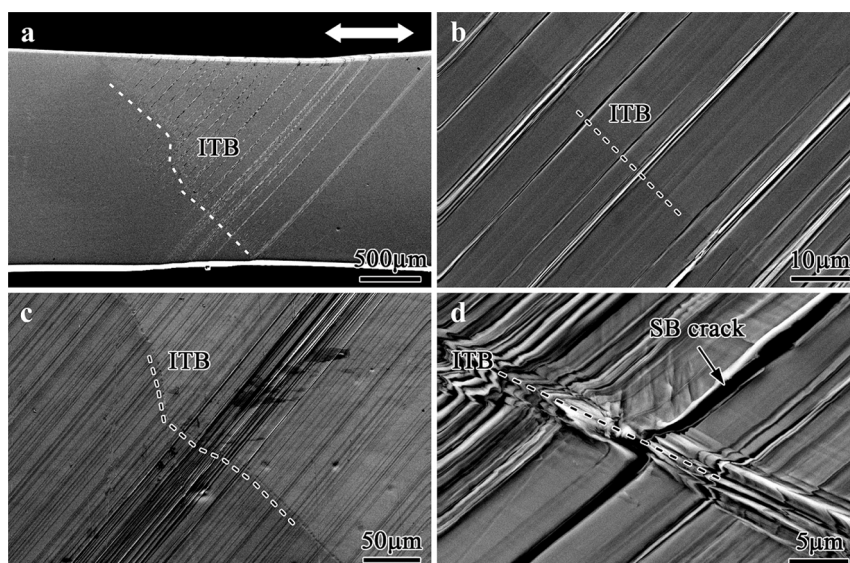

Figure 2 | The surface deformation morphology of the fatigued bicrystal. (a) The macroscopic slip morphology of the bicrystal. (b) Continuous SBs across the straight ITB. (c) Continuous SBs across the curved ITB. (d) The preferential SB crack breaking through the ITB.
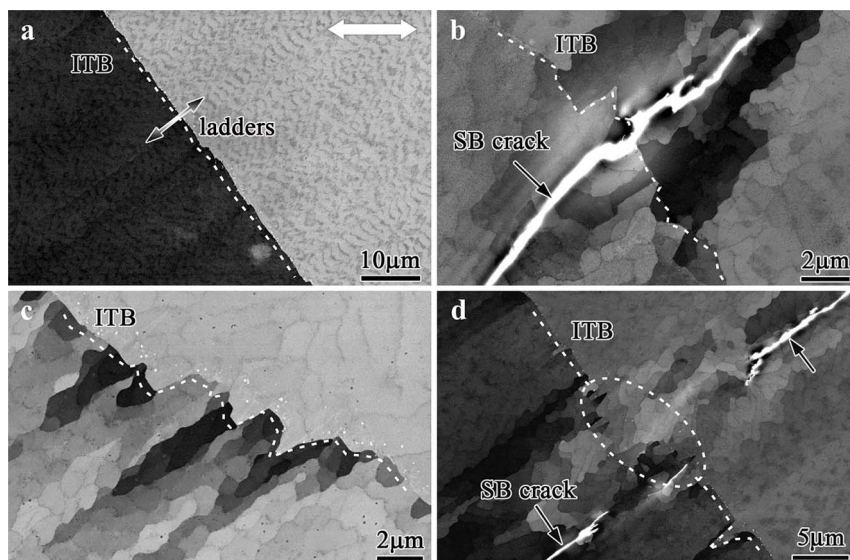
Figure 3 | The subsurface dislocation arrangement of the fatigued bicrystal. (a) Dislocation arrangement near the straight ITB. (b) Dislocation cells surrounding the ITB with a SB crack breaking through the ITB. (c) The microscale curved ITB connected by dislocation cells. (d) Dislocation arrangement near the curved and straight ITB with some indiscernible parts. The white arrow represents the loading direction.

boundary and the black ones represent the lattice full dislocations. The {111} atomic plane in the matrix grain agrees with that in the twin grain every three atomic layers[7,10], thus the ITB is technically penetrable for slips from the component grains though they would also pose limited barrier to the dislocation penetration[20].

On the other hand, the trace of the ITB was verified by electron backscatter diffraction (EBSD) observation. The step size is 50 nm and the confidence is about 99%. The representative IPF + GB maps of the pristine and fatigued ITB are exhibited in Fig. 5a and Fig. 5b respectively with the color showing the out-of-plane orientation of the specimen. It appears that the pristine ITB has fewer and smaller peaks and valleys compared with the fatigued ITB, meanwhile, there might be steps undetected beyond the present resolution. We recorded many heights and widths of the peaks and valleys along the fatigued and pristine ITB as illustrated by the inset of Fig. 5d and the statistic results are summarized in Fig. 5c and Fig. 5d. The heights and widths of the fatigued ITB concentrate at about 1 μm in accordance with the size of dislocation cells, which confirms that the ITB is connected by the dislocation cells. Moreover, the height increases remarkably after fatigue which demonstrates that the migration of ITB does occur during the cyclic deformation. The little change in widths implies that the migration mainly occurs along the slip direction perpendicular to the ITB. Indeed, the ITB has been widely observed to migrate by the motion of partial dislocations especially at the nanoscale under unidirectional loading[13,14,27–29].

In addition, it could be derived from the ECC and EBSD observations that, there is certain difference between the mobility and penetrability of the ITB at different positions. The continuous dislocation ladders across the ITB could be easily observed around the straight ITB which demonstrates that the slip penetration is more prominent at the straight part as sketched in Fig. 6b. In addition, there are abundant coherent steps along the curved ITB. The high resolution TEM image of the fatigued ITB conjunct with CTB steps is shown in Fig. 6a. The ITB also dissociates under cyclic loading and the two white dashed lines represent the two boundaries of the ITB. The separating distance between the two boundaries of the ITB is narrow while it is larger at the ITB-CTB juncture. The partials could glide for a large distance along the CTB plane and the planes parallel to the CTB, which could lead to the ITB migration as sketched in Fig. 6c. That is, the coherent steps facilitate the partials glide and the subsequent boundary migration. And it is proposed that the ITB migration rates showed an inverse dependence on the width of the ITB segment[11]. Under the cyclic push-pull loading, the partials would glide forward or backward collectively and the displacement or velocity of each part differs as illustrated in Fig. 6c, which explains the rough ITB trace induced by fatigue. Meanwhile, it is noted that the ITB migration is more evident at curved part while the slip penetration is more prominent at the straight part and quantitative study needs to be done in future.
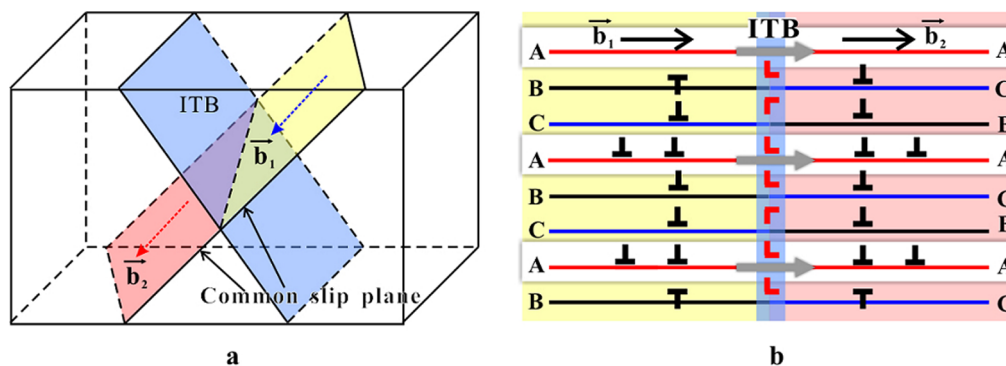

Figure 4 | The schematics for the dislocation penetrating the ITB. (a) The schematic for the primary slip systems of the bicrystal. (b) The interactions between the boundary partial dislocations and lattice full dislocations.
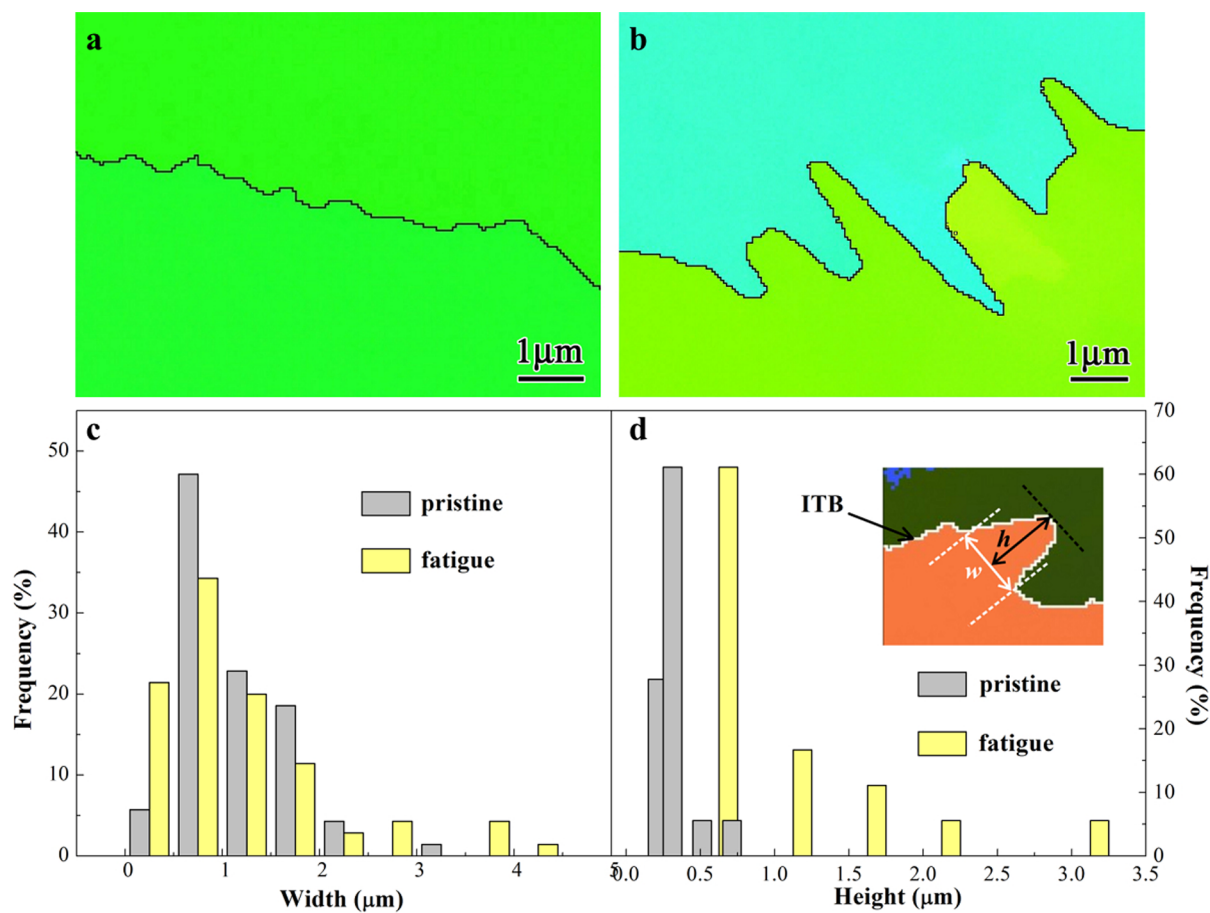
Figure 5 | The EBSD observations of the pristine and fatigued ITB and the statistical results about the sizes of the peaks and valleys along the ITB. (a) The GB + IPF map of the pristine ITB. (b) The GB + IPF map of the fatigued ITB. The statistical results about (c) the heights and (d) the widths of the peaks and valleys along the pristine and fatigued ITB.

Based on the observations above, it could be concluded that the ITB is penetrable and movable during the cyclic deformation which is related to the ITB structure and the special crystallographic orientation. On the one hand, the primary SBs in both of component grains have the same slip planes and slip vectors. Therefore, the slips can pass through the ITB accompanied with good strain compatibility at the ITB. On the other hand, the partial dislocations can easily glide under the applied shear stress which could lead to the ITB migration and relieve the pilling-up stress. In consequence, the SBs bring no damage to the boundary and the little impingement effect can be relieved by the boundary migration during the cyclic deformation. Thus the fatigue cracks nucleated along the SBs preferentially and the ITB showed higher fatigue cracking resistance than the SBs in the present case. The ITB under unidirectional stress has been
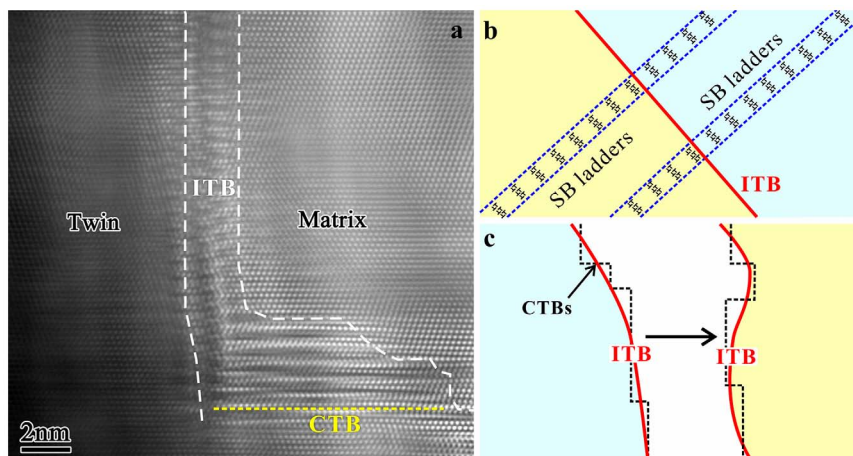

Figure 6 | The high-resolution TEM observation of the fatigued ITB and the sketch for the dislocation penetration and ITB migration. (a) The ITB dissociated during the cyclic deformation and the partials glide large distance along the combined CTB plane. (b) The dislocation penetrating the straight ITB. (c) The rugged ITB formation by the different migration displacements or velocities of different parts.

studied a lot, more experimental and simulation studies are needed urgently for the ITB during the cyclic deformation especially the ITBs have different microstructure from common $\Sigma 3\{112\}$ ITB.

In summary, we revealed the intriguing fatigue cracking mechanism of the Cu bicrystal with an inclined ITB for the first time. It is interesting to find that both the penetrability and mobility of the ITB contribute to its higher fatigue cracking resistance. These findings not only shed light on the role of the penetrable and movable ITB but also could compensate the study on the fatigue cracking mechanisms of a penetrable boundary. It could also provide new and important implications for future interfacial optimization of materials.

Methods

Sample preparation. The bulk bicrystal was grown from oxygen-free high-conductivity Cu of 99.999% purity by Czochralski method. The crystallographic orientation was determined by EBSD. All the fatigue specimens were ground and electro-polished carefully before cyclic deformation.

Experimental methods. The bicrystal specimens were cyclically deformed at room temperature in air and a triangle wave with a frequency of 1 Hz was applied with an Instron E1000 testing machine. Three specimens were applied in the fatigue experiments. Tests in cyclic deformation were conducted under load control. The Cu bicrystals were fatigued with zero mean stress at increased stress amplitude. The shear stress amplitude increased stepwise from 10 MPa to about 30 MPa and after that the shear stress amplitude was kept constant of about 30 MPa. The total strain amplitudes reached at the final stress amplitudes were calculated to be about 1% based on the beam displacement detected by the testing machine. The fatigue specimens were cyclically deformed until fatigue cracks initiated which could be detected by the SEM (scanning electron microscope). The cyclic numbers needed to detect the SB cracks are higher than 7×10^4.

Slip morphology and dislocation arrangement observation. The slip morphologies and fatigue cracks of the specimens were observed by Zeiss Supra-35 SEM. After SEM observation on the surface, the specimens were electro-polished again and examined by ECC imaging technique[16,24] to detect the dislocation arrangement near the ITB.

1. Lu, L., Shen, Y. F., Chen, X. H., Qian, L. H. & Lu, K. Ultrahigh strength and high electrical conductivity in copper. *Science* **304**, 422–426 (2004).
2. Lu, L., Chen, X., Huang, X. & Lu, K. Revealing the maximum strength in nanotwinned copper. *Science* **323**, 607–610 (2009).
3. Lu, K., Lu, L. & Suresh, S. Strengthening materials by engineering coherent internal boundaries at the nanoscale. *Science* **324**, 349–352 (2009).
4. Li, X. Y., Wei, Y. J., Lu, L., Lu, K. & Gao, H. J. Dislocation nucleation governed softening and maximum strength in nano-twinned metals. *Nature* **464**, 877–880 (2010).
5. Wang, Y. M. *et al.* Defective twin boundaries in nanotwinned metals. *Nature Mater.* **12**, 697–702 (2013).
6. Greer, J. R. It's all about imperfections. *Nature Mater.* **12**, 689–690 (2013).
7. Wang, J., Anderoglu, O., Hirth, J. P., Misra, A. & Zhang, X. Dislocation structures of $\Sigma 3$ \{112\} twin boundaries in face centered cubic metals. *Appl. Phys. Lett.* **95**, 021908 (2009).
8. Li, N., Wang, J., Misra, A., Zhang, X., Huang, J. Y. & Hirth, J. P. Twinning dislocation multiplication at a coherent twin boundary. *Acta Mater.* **59**, 5989–5996 (2011).
9. Wang, J. *et al.* Detwinning mechanisms for growth twins in face-centered cubic metals. *Acta Mater.* **58**, 2262–2270 (2010).
10. Lucadamo, G. & Medlin, D. L. Geometric Origin of Hexagonal Close Packing at a Grain Boundary in Gold. *Science* **300**, 1272–1275 (2003).
11. Liu, L., Wang, J., Gong, S. K. & Mao, S. X. High Resolution Transmission Electron Microscope Observation of Zero-Strain Deformation Twinning Mechanisms in Ag. *Phys. Rev. Lett.* **106**, 1775504 (2011).
12. Han, W. Z. *et al.* Deformation and spallation of shocked Cu bicrystals with 3 coherent and symmetric incoherent twin boundaries. *Phys. Rev. B* **85**, 024107 (2012).
13. Brown, J. A. & Ghoniem, N. M. Structure and motion of junctions between coherent and incoherent twin boundaries in copper. *Acta Mater.* **57**, 4454–4462 (2009).
14. Xu, L. H. *et al.* Structure and migration of (112) step on (111) twin boundaries in nanocrystalline copper. *J. Appl. Phys.* **104**, 113717 (2008).
15. Wang, J., Misra, A. & Hirth, J. P. Shear response of 3\{112\} twin boundaries in face-centered-cubic metals. *Phys. Rev. B* **83**, 064106 (2011).
16. Zhang, Z. F. & Wang, Z. G. Grain boundary effects on cyclic deformation and fatigue damage. *Prog. Mater. Sci.* **53**, 1025–1099 (2008).
17. Essmann, U., Gösele, U. & Mughrabi, H. A model of extrusions and intrusions in fatigued metals I. Point-defect production and the growth of extrusions. *Philos. Mag. A* **44**, 405–426 (1981).
18. Kim, W. H. & Laird, C. Crack nucleation and stage I propagation in high strain fatigue-I. Microscopic and interferometric observation. *Acta Metall.* **26**, 777–787 (1978).
19. Zhang, Z. J., Zhang, P., Li, L. L. & Zhang, Z. F. Fatigue cracking at twin boundaries: Effects of crystallographic orientation and stacking fault energy. *Acta Mater.* **60**, 3113–3127 (2012).
20. Li, N., Wang, J., Huang, J. Y., Misra, A. & Zhang, X. Influence of slip transmission on the migration of incoherent twin boundaries in epitaxial nanotwinned Cu. *Scripta Mater.* **64**, 149–152 (2011).
21. Christian, J. W. & Mahajan, S. Deformation twinning. *Prog. Mater. Sci.* **39**, 1–157 (1995).
22. Zhang, Z. F. & Wang, Z. G. Dependence of intergranular fatigue cracking on the interactions of persistent slip bands with grain boundaries. *Acta Mater.* **51**, 347–364 (2003).
23. Thompson, N., Wadsworth, N. & Louat, N. X. The origin of fatigue fracture in copper. *Philos. Mag.* **1**, 113–126 (1956).
24. Zhang, Z. F. & Wang, Z. G. Investigations of dislocation patterns within grains and near grain boundaries in copper by the electron channelling contrast technique in scanning electron microscopy. *Philos. Mag. Lett.* **78**, 105–113 (1998).
25. Li, L. L., Zhang, P., Zhang, Z. J. & Zhang, Z. F. Effect of crystallographic orientation and grain boundary character on fatigue cracking behaviors of coaxial copper bicrystals. *Acta Mater.* **61**, 425–438 (2013).
26. Shen, Z., Wagoner, R. H. & Clark, W. A. T. Dislocation and grain boundary intersections in metals. *Acta Metall.* **36**, 3231–3242 (1988).
27. Wang, Y. B., Sui, M. L. & Ma, E. In situ observation of twin boundary migration in copper with nanoscale twins during tensile deformation. *Philos. Mag. Lett.* **87**, 935–942 (2007).
28. Zhu, Y. T. *et al.* Twinning partial multiplication at grain boundary in nanocrystalline fcc metals. *Appl. Phys. Lett.* **95**, 031909 (2009).
29. Jang, D. H., Li, X. Y., Gao, H. J. & Greer, J. R. Deformation mechanisms in nanotwinned metal nanopillars. *Nature Nanotechnology* **7**, 594–601 (2012).

Acknowledgments

Author contributions

L.L.L. prepared the Cu bicrystals and did the cyclic-deformation experiments. Z.F.Z. conceived the research and provided guidance. L.L.L., P.Z., Z.J.Z. and Z.F.Z. analyzed the data and wrote the manuscript. All authors contributed to the scientific discussions and reviewed the manuscript.

Additional information